



OPEN

Generation of Electromagnetic Waves with Arbitrary Orbital Angular Momentum Modes

SUBJECT AREAS:

ELECTRICAL AND
ELECTRONIC
ENGINEERINGELECTRONIC AND SPINTRONIC
DEVICES

Li Cheng, Wei Hong & Zhang-Cheng Hao

State Key Laboratory of Millimeter Waves, School of Information Science and Engineering, Southeast University, Nanjing 210096, China.

Received
21 January 2014Accepted
8 April 2014Published
28 April 2014Correspondence and
requests for materials
should be addressed to
W.H. (weihong@seu.
edu.cn) or Z.-C.H.
(zchao@seu.edu.cn)

Recently, much attention has been focused on beams carrying orbital angular momentum (OAM) for radio communication. Here we experimentally demonstrate a planar-spiral phase plate (planar-SPP) for generating arbitrary mixed OAM beams. This proposed planar-SPP uses the concept of transmit array antenna having a perforated substrate to control the outputting phase for generating beams carrying OAM with arbitrary modes. As demonstrations, three planar-SPPs with a single OAM mode and two mixed OAM modes around 94 GHz have been investigated with design and experiments in this paper, respectively. The typical experimental intensity and phase patterns show that the proposed method of generating OAM beams really works.

In nowadays, the rapidly developed modern communication systems face serious challenges of improving transmission data-rate due to the limited radio spectrum and polarization even after adopting high density coding and channel sharing techniques. Novel techniques need to be developed for utilizing radio spectrum with very high efficiency. To this end, the orbital angular momentum (OAM) has recently drawn much attention for wireless communications. As been known long before, the electromagnetic waves can carry both linear and angular momentums^{1,2}. Angular momentum comprises spin angular momentum (SAM) and orbital angular momentum (OAM). The SAM is associated with three possible polarization modes of electromagnetic beams, i.e., the left and right circularly polarized modes and linearly polarized mode. These modes can only offer limited channels in communication system. On the contrary, the OAM is related to beam vorticity and phase singularity, which contains a theoretically unlimited range of possibly achievable eigenstates. Since the eigenstates of OAM are mutually orthogonal to each other, they can offer an additional rotational degree of freedom in communication, which can be used as new set of communication channels without increasing the frequency bandwidth³.

The experiment investigated by Allen in 1992 shows that the Laguerre-Gaussian (LG) modes carry an orbital angular momentum of $l\hbar$ per photon, where \hbar is Planck's constant h divided by 2π and l is the OAM mode index⁴. Since then, beams carrying OAM have been successfully employed for widespread applications by lots of researchers in many fields such as astrophysics⁵, optical manipulation⁶, and quantum information⁷. Especially, a remarkable experiment made by Wang in 2012 shows that a more than 1Tbps free space data communication can be achieved by employing orbital angular momentum multiplexing in optical domain. This proved that OAM can be used as a new degree of freedom to improve the spectral efficiency of communication⁸.

However, the majority of the researches and applications of OAM are conducted in the domain of optics; only a few researches on radio beams with OAM have been reported^{3,9,10}. Because OAM is a natural physical property that can be observed in nature in spite of the frequency, it shows bright prospects in terms of the variety of possible applications in radio beams. So it is necessary to investigate OAM generation and detection at radio frequencies.

Beams carrying OAM can be generated in many ways: antenna array^{11,12}, spiral phase plate (SPP)^{10,12}, holographic plate^{10,13} and inhomogeneous birefringent device called "q-plate"¹⁴. Among them, the spiral phase plate (SPP) is one of the common devices generating electromagnetic beams with OAM. In 1996, Turnbull explained how the beams carrying OAM arise from the SPP by using a ray optics model⁹. The thickness of a typical SPP increases in proportion to the azimuthal angle ϕ around the center of the SPP, and keeps constant in the radial direction¹⁵. When the incident plane wave goes through the SPP, the electromagnetic wave will be imprinted on a total phase shift of $2\pi l$ over the full circle. Recently, Bennis simulated a planar antenna to generate an electromagnetic wave carrying OAM by drilling different number of holes in different sectors to form required



outputting phase. The paper only gave the simulated result of single OAM mode and no any mixed OAM modes¹⁶ was reported.

In order to take advantages of the mutually orthogonal eigenstates, some researchers have paid attention to the mixed OAM modes. Wang used four individual SPPs to generate OAM beams with four different OAM modes respectively and designed a non-polarizing beam-splitter to achieve the multiplexing of the OAM beams⁸. And antenna array was employed to generate inter-modulated OAM modes¹². However, to our knowledge, no single antenna has been reported to generate arbitrary mixed OAM modes so far.

In this paper, we experimentally investigated a series of planar OAM antennas to generate arbitrary single-mode and mixed-mode OAM waves by introducing a design method which used transmit array antenna theory. Mixed-mode OAM antennas for generating OAM waves with two superimposed modes and three superimposed modes are studied as demonstration, which can be used to achieve orbital angular momentum multiplexing by using single antenna. Practical electromagnetic wave radiated from an open waveguide is adopted as incident radio wave. The proposed antennas adopted air holes having different radiuses in the substrate, which can directly and conveniently transform the spherical wave to waves with OAM in different states, and can be massive manufactured by using low cost commercial printed-circuit-board (PCB) technology. It is a promising solution to generate OAM waves for future OAM communication system.

Results

Design method of planar-SPP for beams with OAM. As shown in Fig. 1a, we proposed a composite structure including an open-end waveguide and a planar-spiral phase plate (planar-SPP) to generate OAM radio waves, which functions like a transmit array antenna and transforms an incoming phase front into a desired outputting phase front^{17,18}. The open-end waveguide is adopted to provide an incident spherical wave as a primary source, and the proposed planar-SPP is placed parallel to the xy -plane, which transforms the incident waves

to OAM beams. The planar-SPP is a square plane with a length of D , and the distance between the primary source and the planar-SPP is F . Planar quasi-period air holes are drilled in the substrate to form the proposed planar-SPP, which is used to compensate the phase delay associated with incident radio waves from different paths and generates the desired outputting phase distribution.

To simply the analysis, the aperture of the planar-SPP is divided into unit square cells with a side length Δx in both x and y direction, and fixed number of air holes are drilled in each cell as shown in Fig. 1b. As the first step of the design, both the incident and the required outputting phases of all units need to be analyzed. Then compensated phases can be calculated for those units.

Since the Laguerre-Gaussian (LG) modes can carry an OAM of lh per photon and the phase of the electric vector fields in a plane perpendicular to the beam axis has a $l\varphi$ dependence, where l is the OAM mode index and φ is the azimuthal angle¹², the outputting phase of the proposed planar-SPP is designed increasingly in proportion to the azimuthal angle φ around the center of the aperture, which can be expressed as:

$$\text{outphase}(\varphi) = \varphi l \quad (1)$$

Ideally, the incident electromagnetic waves for traditional SPP design are required to be plane waves. However, practical primary sources such as horn antennas and open-end waveguides can only provide spherical wave radiation, especially when they are placed not enough far away from the plate antenna. Hence, there are some unequal phase-distributions need to be compensated on the incident surface of the proposed planar-SPP. The unequal phase distribution can be determined by using a geometrical optics approximation¹⁹ under the assumption that the spherical wave comes from the phase center of the feed:

$$\text{inphase}(\theta) = \frac{2\pi F}{\lambda_0} \frac{1 - \cos(\theta)}{\cos(\theta)} \quad (2)$$

where $\text{inphase}(\theta)$ is the inputting phase of each unit cell, λ_0 is the free-space wavelength of incident spherical wave and F is the distance from surface of the planar-SPP to the phase center of the primary source.

To convert the inputting spherical wave into a spiral-type wave with different modes, each unit of the planar-SPP transforms the inputting phase into the required outputting phase. Then the required compensation phase of each unit can be obtained as a function of coordinate of the xy -plane:

$$\text{phase}(\theta, \varphi) = \text{outphase}(\varphi) - \text{inphase}(\theta) \quad (3)$$

We used a quasi-periodical structure shown in Fig. 1b to transform the incident spherical electromagnetic waves to OAM beams, in which the cell structure is made by four drilled air holes in the substrate. By changing the radius of the air holes, the local effective dielectric constant of the substrate can be adjusted^{20,21}. Then the local refractive index of the substrate, namely n decided by the local effective dielectric constant, can be changed to control the outputting phase. The whole substrate with quasi-periodically drilled air hole cells can be designed to have desired effective dielectric constant distribution with the same thickness. When the incident electromagnetic wave goes through the substrate, desired transmitting phase shifts are achieved. Hence, OAM waves with arbitrary mixed modes can be generated by properly dividing the proposed structure into several small parts to implement individual OAM mode. Unlike the traditional SPPs which require substrate with varied thickness, the proposed planar-SPP can be used to generate arbitrary OAM waves without changing the substrate thickness and keeps in a planar form.

We studied the transmission phase characteristics of the air hole drilled cell at the frequency of 94 GHz. The transmission phase characteristics of the cell are analyzed by considering a unit cell with

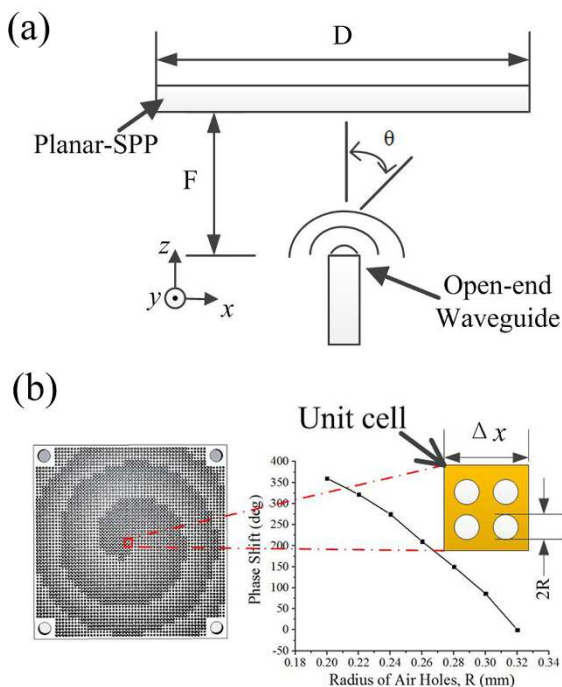


Figure 1 | OAM antenna structure. (a) A side view of an open-end waveguide fed planar-SPP device for an OAM beam application. (b) Units cell used in the design and the phase of transmission coefficient versus air holes radius.

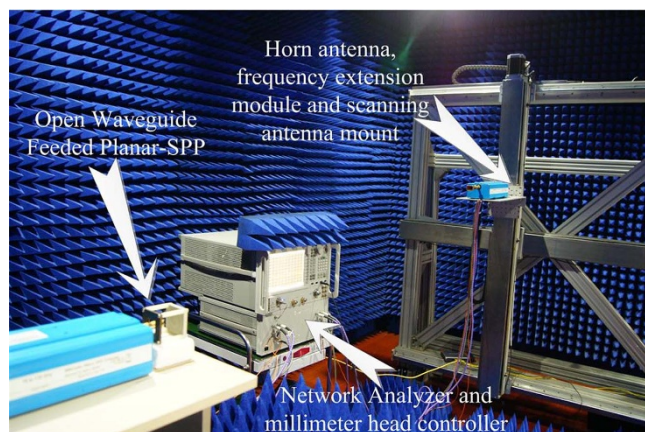


Figure 2 | Measurement setup in an anechoic chamber.

periodic boundary conditions and under a plane wave incidence with the aid of a full-electromagnetic-wave simulation software CST Microwave studio²². The Arlon AD600A substrate is used in the work, which has a dielectric constant of 6.15 and a thickness of 6.35 mm. By simply changing the radius of the four air holes, the corresponding transmitting phase shift is obtained as a function of the radius. As shown in Fig. 1b, the desired transmitted phase shift can be achieved by using unique radius for the drilled air holes. In addition, a phase shifting range exceeding 360 degrees is obtained by adjusting the radius of drilled air holes from 0.2 mm to 0.32 mm, which is enough to realize the arbitrary required phase distribution on the planar-SPP surface. Also, we separate the whole planar-SPP into several sub-parts, and each part is designed respectively taking the method mentioned before to generate electromagnetic wave with a specific OAM mode. In this way, OAM waves with a superposition of multiple OAM modes can be obtained by using only one OAM antenna conveniently.

Experiment results. As demonstrations, we designed three OAM antennas: generating radio beams with OAM mode of $l=1$; superimposed mode of $l=2$ and $l=4$; and superimposed mode of $l=1$, $l=2$ and $l=4$ respectively. All three antennas have the same

aperture size of $D = 45$ mm and are divided into 30×30 unit cells. Each element has a square lattice with a period of 1.5 mm (about 0.47 wavelengths in free space at 94 GHz). And all of the planar-SPPs are illuminated by the same standard W-band rectangular open-end waveguide placed 35 mm away from the planar-SPPs.

The designed prototypes are simulated using CST software and fabricated using commercial printed circuit board (PCB) technology, and measured in an anechoic chamber. The measurement setup is made up of an Agilent PNX Series Network Analyzer 5245A which is equipped with an Agilent millimeter head controller N5161A and two OML WR10 frequency extension modules (75 GHz–110 GHz), a W-band standard horn antenna, and a 2-D electronically controllable scanning stander controlled by a computer, as shown in Fig. 2.

One port of the frequency extension modules is connected to an open-end waveguide to illuminate the planar-SPP and the other port is connected to a standard horn antenna that fixed on the scanning stander to detect the OAM beams. To meet the far-field condition, i.e.

$d = \frac{2D^2}{\lambda_0}$, where D is the aperture dimension of the planar-SPP, the horn antenna is placed 1.3 m away from the planar-SPP.

A program is developed to control the horn antenna scanning on the xy -plane. Then the network analyzer measures the intensity and the phase of the radio beams as a function of the coordinates of the xy -plane. The 94 GHz OAM beams were sampled on a square area of 200×200 grids with a step of 2.5 mm. The intensity and phase can be obtained from the measured transmission scattering parameter at each sampled point. Then the transverse density and phase patterns on xy -plane are plotted using a Matlab code.

Using the equation (3), it is easy to obtain the compensated phase of each cell for $l = 1$ mode. And by employing the design curve in Fig. 1b, the required radius of the air holes in each cell can be obtained. The whole structure is simulated using CST Microwave studio software. The simulated 3-D pattern is shown in Fig. 3b and transverse intensity pattern of the radio beams is presented in Fig. 3c, which shows a typical doughnut-shaped intensity with singularity in the center. The proposed OAM antenna shown in Fig. 3a is manufactured by using PCB technology. Deploying the experiment setup mentioned before, we can obtain both the transverse intensity and phase patterns, which are shown in Fig. 3d and e, respectively. The measured intensity pattern is quite similar to the simulated one as well as the theoretical

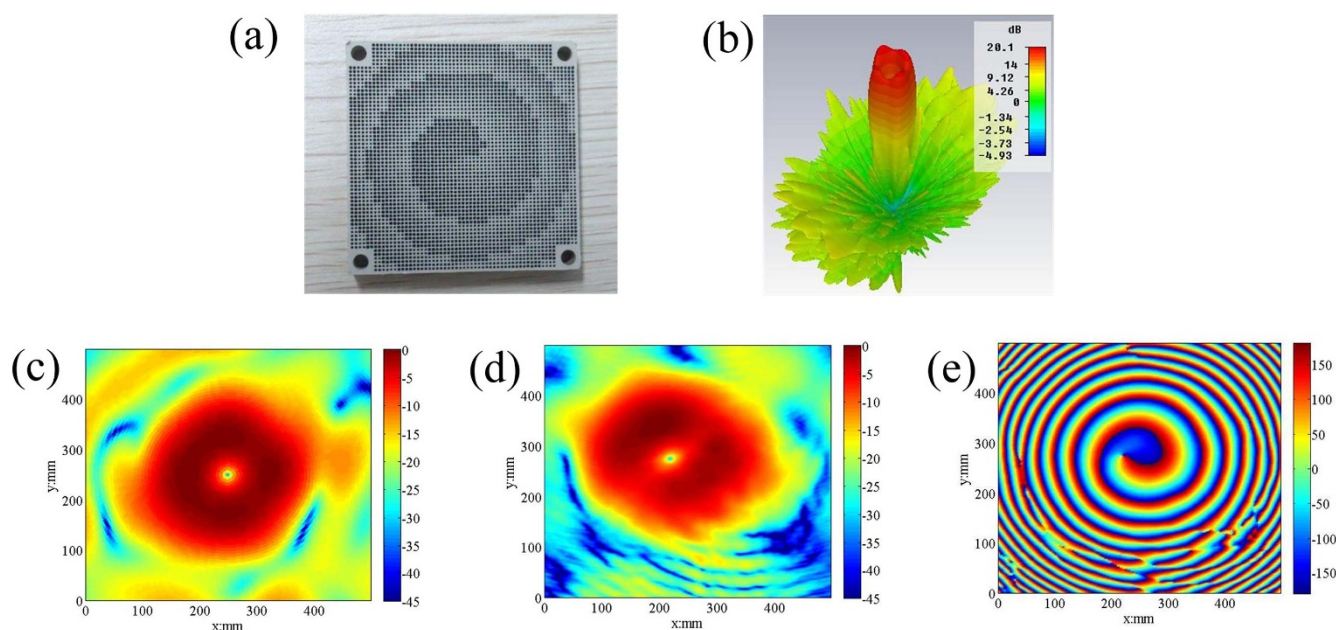


Figure 3 | The simulated and measured results of single mode OAM antenna with state of $l = 1$. (a) The single mode OAM antenna. (b) Simulated 3-D pattern. (c) Simulated transverse intensity pattern. (d) Measured transverse intensity pattern. (e) Measured transverse phase pattern.

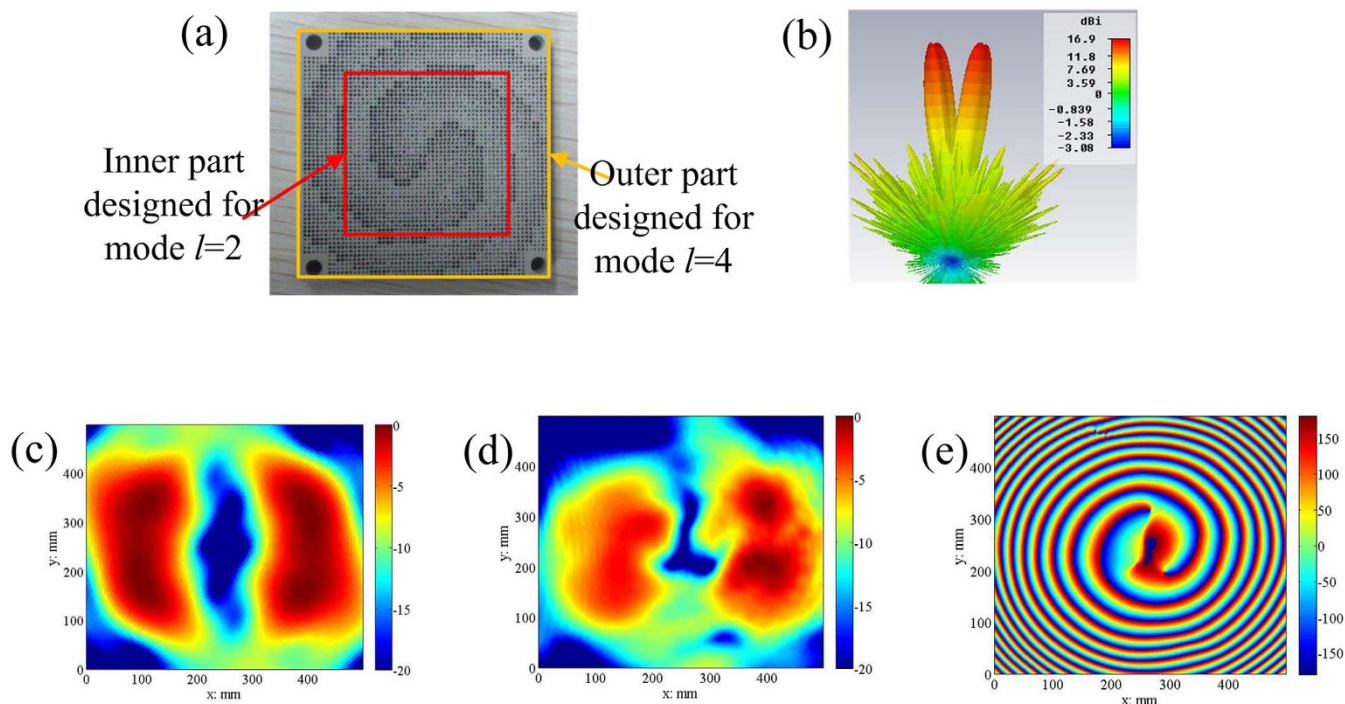


Figure 4 | The simulated and measured results of two-mixed-mode OAM antenna with states of $l = 2$ and 4 . (a) The two-mixed-mode OAM antenna. (b) Simulated 3-D pattern. (c) Simulated transverse intensity pattern. (d) Measured transverse intensity pattern. (e) Measured transverse phase pattern.

result^{12,23}. Also, the experimental phase data shows a total 2π phase change around the centre of the plate as expected.

For superimposed modes of $l = 2$ and $l = 4$, the whole planar-SPP is divided into two parts: the inner and the outer parts. The inner part

is a square area and made up of 20×20 cells in the center of the planar-SPP. This part is designed to generate OAM with a state of $l = 2$. And the outer part is with an annular shape and made up of 500 cells. The outer part is designed to generate OAM with a state of $l = 4$.

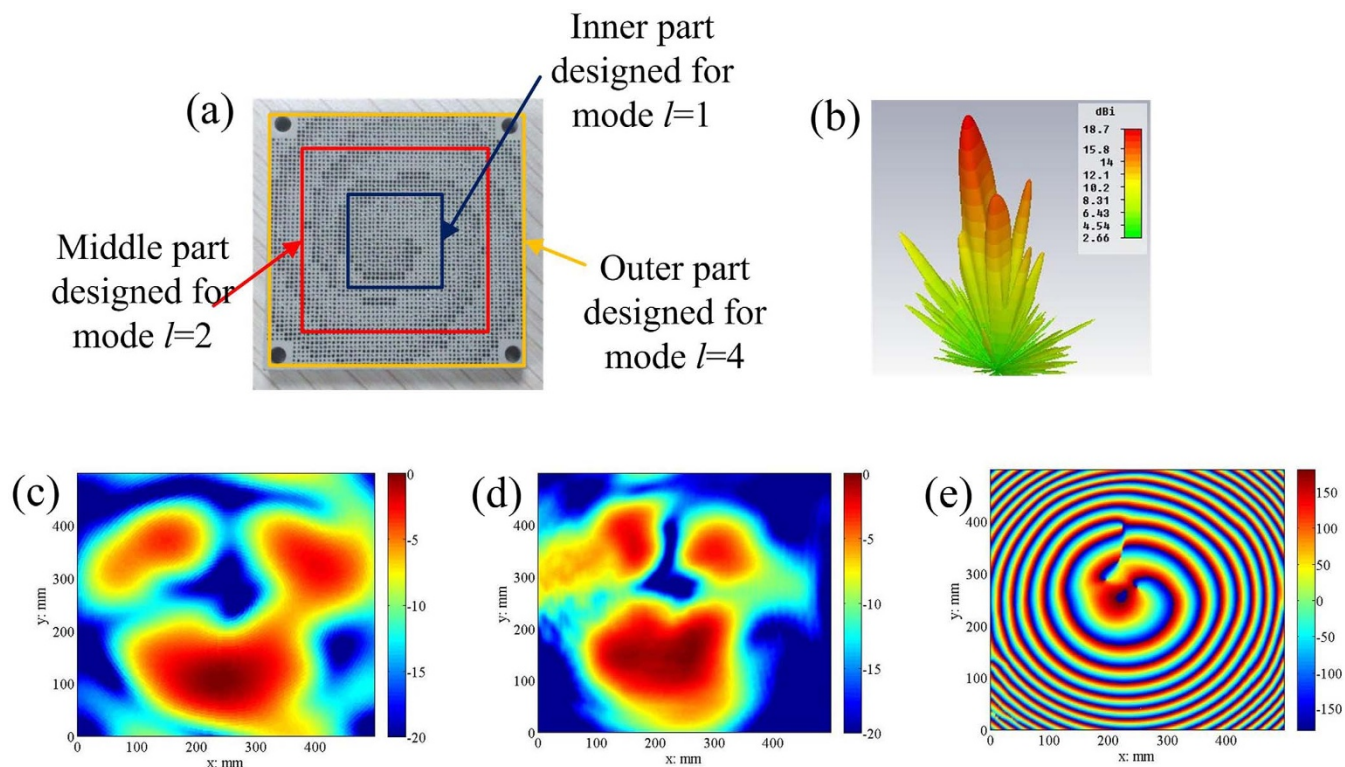


Figure 5 | The simulated and measured results of three-mixed-mode OAM antenna with states of $l = 1$, $l = 2$ and 4 . (a) The three-mixed-mode OAM antenna. (b) Simulated 3-D pattern. (c) Simulated transverse intensity pattern. (d) Measured transverse intensity pattern. (e) Measured transverse phase pattern.



Both parts are designed following the equation (3) and then the compensated phase of each cell for the two modes can be obtained easily. Similarly, the radiuses of the air holes on each element are designed using the curve in Fig. 1b, as shown in Fig. 4a. The simulated 3-D intensity pattern is presented in Fig. 4b, and both the simulated and the measured transverse intensity patterns of the two-mode-antenna are presented in Fig. 4c and d, respectively, where opposite crescent-shaped intensity patterns can be found and they agree well with theoretical analysis¹². Also, the measured transverse phase pattern is presented in Fig. 4e.

The proposed antenna can be designed to generating mixed-mode OAM waves with arbitrary number of OAM states. For example, to design a OAM antenna having superimposed mode of $l = 1$, $l = 2$ and $l = 4$, a planar-SPP is designed by using 900 unit cells which is divided into three parts: the inner, the middle and the outer parts. The inner part is a square and made up of 14×14 cells in the center of the planar-SPP, which is used to generate OAM with the state of $l = 1$. The middle part is with an annular shape and consists 288 cells for generating OAM with the state of $l = 2$. And the outer part is also with an annular shape and consists the last 416 cells for generating OAM with the state of $l = 4$. All the three parts are designed following the equation (3) and then the compensated phase of each cell for the three-mode-antenna can be obtained correspondingly. Again, by applying the curve in Fig. 1b, the whole structure is finalized, as shown in Fig. 5a. The simulated 3-D and the transverse intensity patterns of the three-mode-antenna are presented in Fig. 5b and c. To our knowledge, it is the first report for generating three-mixed-mode OAM waves using single antenna. The proposed structure is also been manufactured using PCB technology and measured in the anechoic chamber. Measured results are illustrated in Fig. 5d and e, respectively. As expectations, well agreements between measured and simulated results are found in Fig. 5.

It can be seen from Figure 3-5 that measured intensity and phase maps of single OAM mode antenna and mixed-mode antenna are much coincided with the theoretical results. That verifies the proposed planar-SPPs have a distinct behavior of OAM beams and can be used to generate beams carrying OAM with any number of desired mixed modes. It shows great prospect in future OAM applications such as high speed communication with a narrow radio frequency band.

Discussion

We have successfully generated electromagnetic beams with OAM of different states by proposing a new concept of planar-SPP. The proposed planar-SPPs employs the concept of transmit array antennas, which use phase shifting elements to obtain the required outputting phase and convert spherical wave into spiral type wave directly. It is a convenient and direct way to generate beams carrying OAM. To our knowledge, it is the first work that shows the experimental intensity and phase results of beams carrying mixed OAM modes. And this work will greatly promote the study and application of OAM in radio frequencies.

Methods

The electromagnetic waves with arbitrary mixed OAM modes are realized by transmitting spherical wave through a planar-SPP. The planar-SPP is manufactured by drilling air holes on a 6.35-mm Arlon AD600A substrate using PCB technology.

The measurement setup is based on an Agilent PNX Series Network Analyzer 5245A, and both phase and magnitude of the electromagnetic waves with arbitrary mixed OAM modes can be measured.

1. Poynting, J. H. The wave motion of a revolving shaft, and a suggestion as to the angular momentum in a beam of circularly polarised light. *Pro. R. Soc. Lond.* **A 82**, 560–567 (1909).
2. Beth, R. Mechanical detection and measurement of the angular momentum of light. *Phys. Rev.* **50**, 115–125 (1936).

3. Tamburini, F. *et al.* Encoding many channels on the same frequency through radio vorticity: first experimental test. *New J. Phys.* **14**, 033001 (2012).
4. Allen, L., Beijersbergen, M. W., Spreeuw, R. J. C. & Woerdman, J. P. Orbital angular momentum of light and the transformation of Laguerre-Gaussian modes. *Phys. Rev. A* **45**, 8185–8190 (1992).
5. Berkhout, G. C. & Beijersbergen, M. W. Method for probing the orbital angular momentum of optical vortices in electromagnetic waves from astronomical objects. *Phys. Rev. Lett.* **101**, 100801 (2008).
6. Cojoc, D. *et al.* Laser trapping and micro-manipulation using optical vortices. *Microelectron. Eng.* **78**, 125–131 (2005).
7. Nagali, E. *et al.* Quantum information transfer from spin to orbital angular momentum of photons. *Phys. Rev. Lett.* **103**, 013601 (2009).
8. Wang, J. *et al.* Terabit free-space data transmission employing orbital angular momentum multiplexing. *Nature Photon.* **6**, 488–496 (2012).
9. Turnbull, G., Robertson, D., Smith, G., Allen, L. & Padgett, M. The generation of free-space Laguerre-Gaussian modes at millimetre-wave frequencies by use of a spiral phaseplate. *Optics Comm.* **127**, 183–188 (1996).
10. Mahmoudi, F. E. & Walker, S. D. 4-Gbps Uncompressed Video Transmission over a 60-GHz Orbital Angular Momentum Wireless Channel. *IEEE Wireless Comm. Lett.* vol 2, 223–226 (2013).
11. Mohammadi, S. M. *et al.* Orbital angular momentum in radio—a system study. *IEEE Trans. Antennas Propag.* vol. **58**, 565–572 (2010).
12. Thidé, B. *et al.* Utilization of photon orbital angular momentum in the low-frequency radio domain. *Phys. Rev. Lett.* **99**, 087701 (2007).
13. Capasso, F., Genevet, P., Lin, J. & Kats, M. A. Holographic Detection of the Orbital Angular Momentum of Light With Plasmonic Photodiodes. *Nature Comm.* **3**, 1278 (2012).
14. Maccalli, S. *et al.* Q-plate for millimeter-wave orbital angular momentum manipulation. *Appl. opt.* **52**(4), 635–639 (2013).
15. Uchida, M. & Tonomura, A. Generation of electron beams carrying orbital angular momentum. *Nature* **464**, 737–739 (2010).
16. Beniss, A., Niemiec, R., Brousseau, C., Mahdjoubi, K. & Emile, O. Flat plate for OAM generation in the millimeter band. Flat plate for OAM generation in the millimeter band. *European Conference on Antennas & Propagation (EUCAP)*2013, Sweden.
17. Pozar, D. Flat lens antenna concept using aperture coupled microstrip patches. *Electron. Lett.* **32**, 2109–2111 (1996).
18. Gagnon, N., Petosa, A. & McNamara, D. A. Thin microwave quasi-transparent phase-shifting surface (PSS). *IEEE Trans. Antennas Propag.* vol **58**, 1193–1201 (2010).
19. Gagnon, N., Petosa, A. & McNamara, D. A. Research and Development on Phase-Shifting Surfaces (PSSs). *IEEE Antennas Propag Mag.* **55**, 29–48 (2013).
20. Abd-Elhady, M., Hong, W. & Zhang, Y. A Ka-Band Reflectarray Implemented With a Single-Layer Perforated Dielectric Substrate. *IEEE Antennas Wireless Propag. Lett.* **11**, 600–603 (2012).
21. Colburn, J. S. & Rahmat-Samii, Y. Patch antennas on externally perforated high dielectric constant substrates. *IEEE Trans. Antennas Propag.* vol **47**(12), 1785–1794(1999).
22. CST Microwave Studio, www.cst.com, 2013.
23. Mohammadi, S. M. *et al.* Orbital angular momentum in radio: Measurement methods. *Radio Science*, **45**(4) (2010).

Acknowledgments

The authors thank H.Z., X.-C. Z., M.J. and S.-H. Y. in the state key lab of millimeter-waves, southeast university, China, for their stimulating discussions. The authors acknowledge the funding support from National Basic Research Program of China, the 973 program 2010CB327400.

Author contributions

W.H. proposed the method. Z.-C.H. and L.C. developed the method. L.C. set up the experiments. All the authors performed the experiments and analysis. Z.-C.H. and L.C. wrote the main manuscript text. All authors discussed the results and commented on the manuscript.

Additional information

Competing financial interests: The authors declare no competing financial interests.

How to cite this article: Cheng, L., Hong, W. & Hao, Z.-C. Generation of Electromagnetic Waves with Arbitrary Orbital Angular Momentum Modes. *Sci. Rep.* **4**, 4814; DOI:10.1038/srep04814 (2014).



This work is licensed under a Creative Commons Attribution-NonCommercial-NoDerivs 3.0 Unported License. The images in this article are included in the article's Creative Commons license, unless indicated otherwise in the image credit; if the image is not included under the Creative Commons license, users will need to obtain permission from the license holder in order to reproduce the image. To view a copy of this license, visit <http://creativecommons.org/licenses/by-nc-nd/3.0/>